TURBULENT BUDGETS IN ROTATING PIPES BY DNS

Paolo Orlandi & David Ebstein
Università di Roma "La Sapienza"
Dipartimento di Meccanica e Aeronautica
via Eudossiana 18 00184 Roma
Italy.

ABSTRACT

The budgets for the Reynolds stresses are given for a non-rotating and a rotating pipe at high rotation rates. The data have been obtained by fields generated by direct numerical simulations at $Re = 4900$. Particular emphasis has been devoted to the near wall region since background rotation modifies the wall structures. These budgets are useful to whom is interested to develop new one-point closure turbulence models for rotating flows.

INTRODUCTION

The study of turbulent flows through a pipe rotating about its axis is of fundamental interest for several flows in practical applications. Some are of engineering interest, such as the study of combustors, rotating machinery or applications connected to aeroacoustic. In addition, rotating flows occur in geophysical applications. The effects of solid body rotation on turbulence in a pipe presents similarities with three-dimensional boundary layers of practical importance, such as on swept wings of airplanes.

When a fluid enters a pipe rotating about its axis, tangential shear forces, acting between the pipe wall and the fluid, cause the fluid to rotate with the pipe, resulting in a flow pattern rather different from that observed in a stationary pipe. Rotation was found to have a very marked influence on the suppression of the turbulent motion because of centrifugal forces. The influence of rotation on the flow may be interpreted as a body force which can stabilize or destabilize turbulence. Experimental results by Nishibori *et.al*(1987) and Reich & Beer (1989) indicate that the rotation changes the mean axial velocity profile tending towards the parabolic profile characteristics of laminar flows. In addition there is the creation of a mean azimuthal velocity, in the reference frame of the rotating pipe, that makes this flow no any longer unidirectional. This component, negligible from the engineering point of view, is a good indicator of the performances of turbulence models. Hirai *et.al*(1988) for instance showed that standard $K - \epsilon$ can not produce this velocity profile. From the physical point of view however a definite answer whether this component is Reynolds and rotation number independent still has not been reached.

Although a lot of experimental work has been done on turbulent rotating pipes, up to values of $N = 5$, a lot less has been achieved numerically. Recently large-scale computers enabled direct numerical simulations of such flows. In addition, the numerical simulation of turbulent pipe flows has received less interest than the turbulent channel, because of the numerical difficulties in treating the singularity at the axis. However, our opinion is that the rotating pipe, even if necessitates of some attention on the numerics, on the other hand, avoids assumptions on the spanwise dimension in a channel rotating along an axis directed in the streamwise direction. In fact, in this case, the spanwise dimension should account for the formation of the large scale rolls at the center of the channel. The pipe has the further advantage to perform comparisons with laboratory experiments. To our knowledge experiments for the rotating channel did not appear in literature, and, to our opinion, they should be very difficult to realize.

Orlandi & Fatica (1997) performed simulations for a rotating pipe for values of the rotation number N up to 2, and showed that the changes in turbulence statistics are due to the tilting of the near-wall streamwise vortical structures in the direction of rotation. The present study is an extension of the previous one by increasing N in the range between 2 and 10, in order to examine numerically the phenomena observed experimentally by Nishibori *et.al*(1987). They measured some of the Reynolds stresses at different values of N. These profiles, however, were mainly evaluated near the entrance of the pipe ($L_e/D < 100$) and not in the fully developed region. To our knowledge, no detailed experimental data on the Reynolds stresses are available yet for fully developed flows at high N. The other main objective of the present work lies in the evaluation of the Reynolds stress budgets, a very easy task by the data from DNS.

Although in simple flows, eddy viscosity models produce results comparable to those by Reynolds-stress models, the latter are necessary in a variety of flows that simpler models ($k - \epsilon$) could not describe. The turbulent rotating pipe is one of them. Hirai *et.al* (1988) proved that the conventional $k - \epsilon$ model does not work for this flow. Even the Durbin (1991) model does not account for the rotation ef-

fects in the outer region of the pipe, whose effects could perhaps be modeled as suggested by Zeman (1995). However it is always more urgent to develop reliable Reynolds-averaged models for industries interested to design more efficient turbomachines.

The Reynolds stress equations contain several terms that must be modeled and that are difficult to measure. For instance, the pressure-strain correlation tensor, that for certain stresses is comparable to the production term, and to the rate of dissipation. Therefore, it is necessary to obtain these terms numerically.

It is proposed here to study the phenomena occurring in the rotating pipe at high speed of rotation by evaluating the Reynolds stresses budgets and examining their dependence on N. The Reynolds number of the direct simulation is much smaller than that considered with one-point closures. LES were performed by Eggels *et.al* (1994) but these were limited at low N. Our point of view is that, to have reliable turbulence model for the rotating pipe the near wall region should be considered. In the past, for the turbulent channel (Mansour *et.al* 1989), the DNS at low Reynolds number was of great help to the turbulence modelers (Durbin 1991), thus, we think that, even more for this complex flow, the low Reynolds DNS should be of great help to model the wall region, and in particular at high rotation rates.

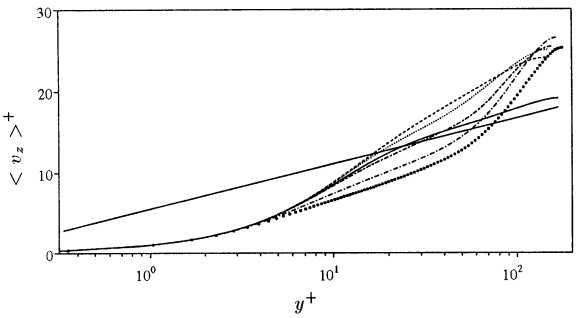

FIGURE 1. Velocity profile in wall units (—— $N = 0$), (---- $N = 0.5$), (····· $N = 1$), (—·— $N = 2$), (—··— $N = 5$), (• • • • • $N = 10$).

EQUATIONS

The dimensionless Navier-Stokes equations in a reference frame rotating with the pipe wall are

$$\frac{D\mathbf{U}}{Dt} = -\nabla p + \frac{1}{Re}\nabla^2\mathbf{U} + N\mathbf{e_z} \times \mathbf{U} \qquad (1)$$

where it has been assumed that the rate of rotation Ω is direct along the versor $\mathbf{e_z}$. The dimensionless equations have been obtained by taking the pipe radius R as reference length, the laminar Poiseuille velocity U_P, twice the bulk velocity U_b, as velocity scale. These quantities together with the kinematic viscosity ν give $Re = U_b D/\nu = U_P R/\nu$ and the rotation number $N = \Omega R/U_b$.

These equations can be solved when boundary conditions are assigned. This paper deals with a flow inside a circular pipe, hence no-slip conditions are assumed on the wall. Being interested to the statistical steady state, periodicity is assumed along the streamwise direction. The second order finite difference scheme in space and time developed by Verzicco & Orlandi (1996) is briefly reported in Orlandi & Fatica (1996) where in the Appendix the grid refinement checks were discussed. In that study the simulations were done up to $N = 2$; here the calculations have been extended to higher rotation rates $N = 5$ and $N = 10$. The results presented here are achieved by a $129 \times 96 \times 193$ grid. In a longer report by Ebstein (1998) it is shown that do not largely differ from those obtained by a coarser grid. In simulations of rotating pipes an important choice is the length of the pipe, that should be long enough to capture the stretching of the vortical structures due to the rotation rate as observed in the experiments by Nishibori *et.al* (1987). In all the simulations with $N > 0$ it was assumed $L_z/R = 25$, while for that at $N = 0$ L_z/R wat set equal to 15.

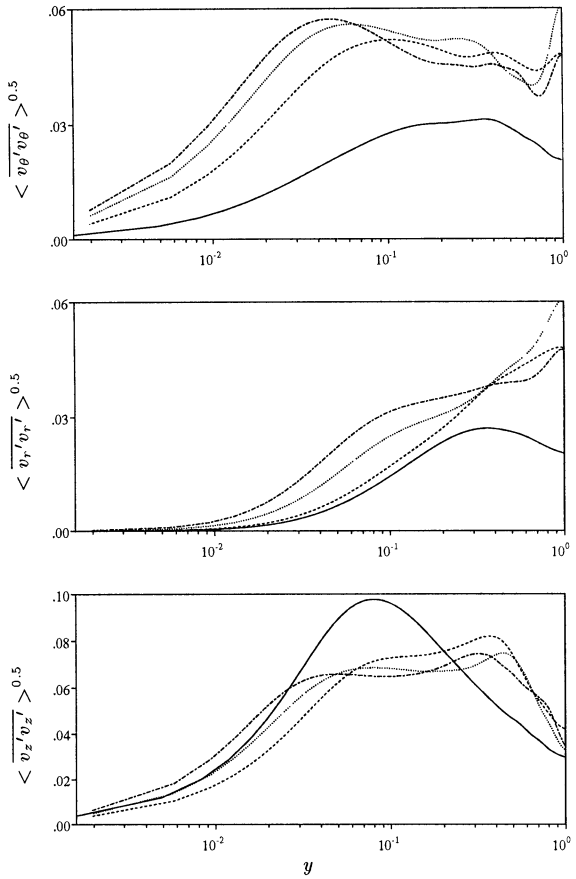

FIGURE 2. Normal stress profiles (—— $N = 0$), (---- $N = 2$), (····· $N = 5$), (—·— $N = 10$).

Approximately 60 fields separated by two time units were saved and by a post-processing code the statistics and the budgets were evaluated. In all the quantities reported here the overline accounts for time averages and $<>$ for averages in the azimuthal and streamwise direction. In Fig.1 the $< v_z >$ profiles in wall units, in addition with those at $N = 0.5$ and $N = 1$, show that by increasing N the log region is not any more present, indicating that turbulence models based on the law-of-the-wall should be discarded. The profiles of $< v_\theta >$ are not reported, but it has been observed that the correction with respect to the solid body rotation decreases by increasing the rotation rate. In the experiments up to $N = 5$ by Reich & Beer (1989) the profile was independent from N and Re. However in more recent experiments by Imao *et.al* (1996) at $N = 0.5$ and $N = 1$ the data do not perfectly coincide with the theoreti-

cal parabolic profile and in addition are slightly separated. In our simulation has been checked that at any N in the equation for $< \overline{v_\theta} >$ and $< \overline{v_r} >$, where the terms with $< \overline{v_\theta} >$ appear the balance was satisfied. From these arguments a definite answer on the profile of $< \overline{v_\theta} >$ can not be drawn, more experiments and more refined simulations are requested.

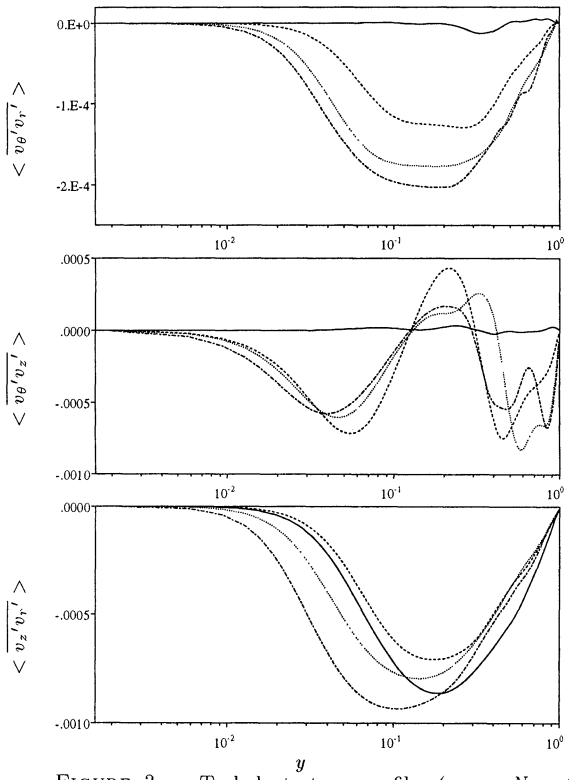

FIGURE 3. Turbulent stress profiles (——— $N = 0$), (---- $N = 2$), (····· $N = 5$), (—·— $N = 10$).

At low N the measurements by Imao *et.al* (1996) show that the normal stresses in the region far from the wall do not vary appreciably with the rotation, and this is confirmed by the simulations, even if in the DNS a substantial drop between $N = 0$ and $N = 0.5$ occurs near the wall. The condition is rather different at very high rotation rates. This is shown in Fig.2 where the normal stresses profiles, normalized with respect to U_P, are shown. The profiles are not given in wall coordinates since the variation of friction velocity with N will not clearly show their increase or reduction. At these high values of N the normal stresses are affected in the wall and in the outer region and in particular near the center of the pipe. $< \overline{v_\theta' v_\theta'} >^{0.5}$ increases everywhere. Also $< \overline{v_r' v_r'} >^{0.5}$ increases, but near the wall less than near the central region of the pipe. $< \overline{v_z' v_z'} >^{0.5}$ on the other hand decreases near the wall and increases at the center. We would like to point out that the profiles in a semilog scale emphasize the near wall region. This choice is of particular utility when the DNS should guide the modeling of the wall region. As a general results we observe that the rotation moves the peak of the turbulent kinetic energy from the wall towards the center of the pipe.

More drastic modifications occur for the turbulent stresses, in fact the rotation, braking the symmetry, produces the stresses that are null in the non-rotating pipe. These stresses are given in Fig.3a-c and in particular it turns out that $< \overline{v_\theta' v_z'} >$ is large and that it oscillates between positive and negative values. These oscillations, almost absent at low rotation rates, are a consequence of the long spiral structures forming in the central region of the pipe. These stresses were measured by Imao *et.al* (1996) at low rotation rate at $Re = 20000$ four times bigger than the present ($Re = 4900$). Fig.4 shows that, although there are differences between the numerical and experimental results, nevertheless the decrease of $< \overline{v_\theta' v_z'} >$ with N and the locations of sign change are reasonably well predicted. On the other hand, the large differences for $< \overline{v_z' v_r'} >$ should be attributed to the differences in Reynolds number. In fact Orlandi & Fatica (1997) showed that the profile of the total stress follows the theoretical linear behavior and that the reduction of the pressure drop is not linear in N, differently than in Imao *et.al* (1996). The simulations at higher Reynolds number in principle could be done with the todays computers; this will be done, in the near future, to generate a new database at $N = 0.5$ and $N = 1$, since we did not save the fields for the low values of N. The database at the higher values of N has been used to evaluate the budgets, described in the next section.

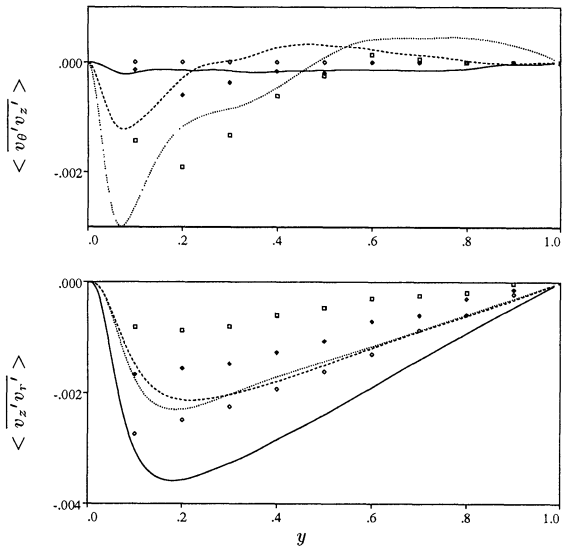

FIGURE 4. Turbulent stress profiles compared with the Imao *et.al*(1996) data (——— $N = 0$), (---- $N = 0.5$), (····· $N = 1$).

BUDGETS

Hirai *et.al* (1987) proved that the conventional $k - \epsilon$ model does not work and hence for rotating pipes the second order closure should be used. This statement suggests to consider the equation of the Reynolds stresses, that at the steady state, and in the fully developed conditions, can be schematized as

$$< \overline{u_k} > \frac{\partial R_{ij}}{\partial x_k} = -R_{ik}\frac{\partial < \overline{u_j} >}{\partial x_k} - R_{jk}\frac{\partial < \overline{u_i} >}{\partial x_k} + \nu\nabla^2 R_{ij} + \Pi_{ij} - \epsilon_{ij} - \frac{\partial S_{ijk}}{\partial x_k} - 2(e_{mki}\Omega_m R_{jk} + e_{mkj}\Omega_m R_{ik}) \quad (2)$$

The expression in cylindrical coordinates are not given, these are reported in literature and can be found in Ebstein (1998). The Reynolds stresses are defined as

$R_{ij} = < \overline{u_i' u_j'} >$, in $S_{ijk} = < \overline{u_i' u_j' u_k'} >$ only the triple velocity correlations appear and $\Pi_{ij} = < \overline{u_i' \frac{\partial p'}{\partial x_j} + u_j' \frac{\partial p'}{\partial x_i}} >$. The rate of dissipation is $\epsilon_{ij} = 2\nu < \overline{\frac{\partial u_i'}{\partial x_k} \frac{\partial u_j'}{\partial x_k}} >$. Equation (2), by inserting the Coriolis inside the convective term, in a more compact way can be written, as

$$0 = PD + VD + VP + DS + TD + CT \qquad (3)$$

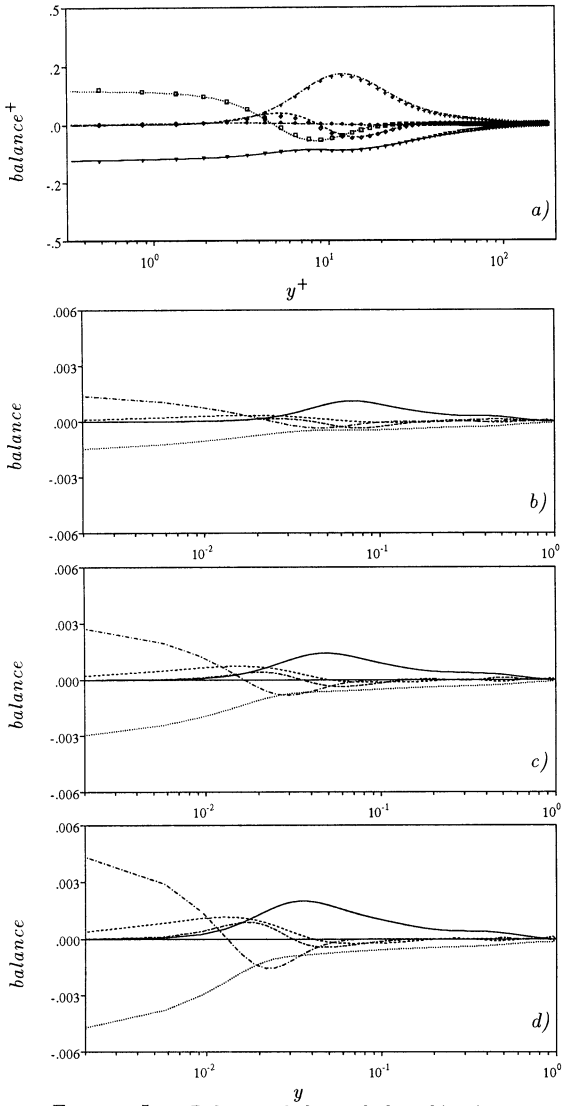

FIGURE 5. Balance of the turbulent kinetic energy in a) the symbols are from Mansour *et.al*(1988); the data are normalized with respect to νu_τ^4, b) $N = 2$, c) $N = 5$, d) $N = 10$ in the dimensionless units of the simulations. (—— PD), (---- VP), (····· DS), (— — TD). (—·— VD).

PD indicates production, VD viscous diffusion, VP the correlation between velocity and pressure gradients, DS the rate of turbulent dissipation, TD the turbulent diffusion and CT the convective term. The balance usually are normalized with respect νu_τ^4; in dimensionless units it means that each term of equation (2) should be divided by Reu_τ^4. To whom is interested to transform the data we would like to recall that $Re = 4900$ and that for the four N, u_τ respectively is 0.03475, 0.03214, 0.03405 and 0.0369. From these values it turns out that, differently than expected, by increasing N there is a drag reduction up to $N = 2$ and then a drag increase. Nevertheless the mean velocity profile tends to the laminar parabolic profile in the internal region of the pipe.

The budget for the turbulent kinetic energy at $N = 0$ agrees perfectly with the budget by Mansour *et.al* (1988) for the plane channel as it is shown in Fig.5a, by the results normalized with respect to Reu_τ^4. In the turbulent kinetic energy equation does not directly appear the effect of the solid body rotation but Fig.5 shows which are the terms more affected by the rotation. For these terms it is interesting to investigate how each Reynolds stress behaves. Once more it is important to remember that the simulations at low Reynolds number help to model the whole region of the pipe. Fig.5 shows that, indeed, in the viscous region there is a large growth of the rate of dissipation (DS) and as a consequence of the viscous diffusion (VD) balancing it. The turbulence production (PD) and the turbulent diffusion (TD) are less affected by N. The turbulent production for K coincides with the production term in the $< \overline{v_z' v_z'} >$ equation, where N does not appear, and hence the changes in production with N are indirec. The production term in the other two normal stresses cancel each other and their profiles show that the largest values occur in the log region contributing to the increase of the stresses with N, near the center, depicted in Fig.2. The analogous of Fig.5 for each stress can be found in Ebstein (1998).

Fig.5 shows a large change of the rate of dissipation, hence it is interesting to investigate whether the assumption, usually done in second order closures at high Reynolds numbers, that $\epsilon_{ij} = \epsilon \delta_{ij}$ is valid or not. In Fig.6 the profiles of the ϵ_{ij}^+ for each N are given. Who is interested can eliminate the u_τ dependence by using the values previously given. About the possibility that $\epsilon_{ij} = \epsilon \delta_{ij}$ is valid at high and not a low Re we investigated, from the data of the channel in Rodi & Mansour (1993), that by increasing by a factor of two the Reynolds number the profiles of ϵ_{ij}^+ indeed do not change. Fig.6 clearly shows that the local isotropy assumption is not valid, and that, irrespective of N, ϵ_{rr} is always much smaller than the other two rate of dissipation. The rate of dissipation of the turbulent stresses are smaller than those of the normal stresses, but by increasing N, in the wall region, $\epsilon_{\theta z}^+$ increases. It is interesting even to notice that only for $< \overline{v_\theta' v_z'} >$ the near wall region is important, for the other two ($< \overline{v_z' v_r'} >$ and $< \overline{v_\theta' v_r'} >$) in the wall region the rate of dissipation is smaller than that near the center of the pipe.

The balance for each turbulent stress shows that the terms largely dependent on the rotation rate are the velocity pressure gradient correlation and the convective term, that becomes large for the direct contribution of N. In Eq.(3) for the turbulent stresses has been observed that $CT + VP$ is balanced by PR. As before mentioned the numerical data should help on modeling the VP term, hence we are presenting only for $N = 2$ the plots of this term splitted in the pressure strain and in the pressure transport terms together with CT. We would like to point out that at $N = 10$ VP and CT are of opposite sign and each one is much greater than the other terms. $VP + CT$, on the other hand, is comparable to the others, hence if each term is not appropriately modeled it could produce erroneous results. In Fig.7 PS indicates the pressure strain correlation, usually modeled explicitly in the second order closure, and for which the most used closure was done by Launder, Reece & Rodi (1975). PD is the pressure transport term, usually included in the turbulent diffusion, that has the constraint of a null integral. Fig.7a shows that,

near the wall, in the equation for $< \overline{v_\theta' v_\theta'} >$, PS and PD balance and hence VP is negligible; in the outer region VP is similar to CT and of opposite sign. CT prevails on VP and then both give a positive contribution to the production of $< \overline{v_\theta' v_\theta'} >$ and it explains why $< \overline{v_\theta' v_\theta'} >$ increases in the central part of the pipe by increasing N. Fig.7b shows that in the equation for $< \overline{v_r' v_r'} >$ CT has an opposite sign than in the $< \overline{v_\theta' v_\theta'} >$ equation and that it differs from PV; $CT + PV$ contributes to increase $< \overline{v_r' v_r'} >^{0.5}$ in the wall region has it is shown in Fig.2a.

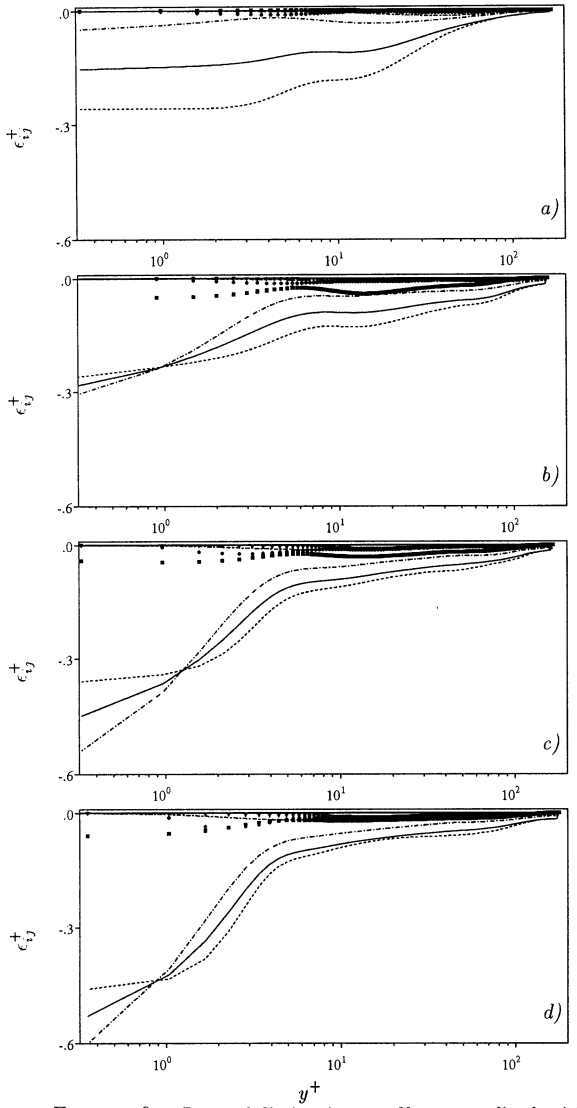

FIGURE 6. Rate of dissipation profiles normalized with respect to νu_τ^4in function of y^+; in a) $N = 0$ b) $N = 2$, c) $N = 5$, d) $N = 10$. (—— ϵ), (---- ϵ_{zz}), (—-— $\epsilon_{\theta\theta}$), (—·— ϵ_{rr}), ($\triangle$ $\epsilon_{\theta r}$), ($\bullet$ ϵ_{zr}), ($\square$ $\epsilon_{\theta z}$).

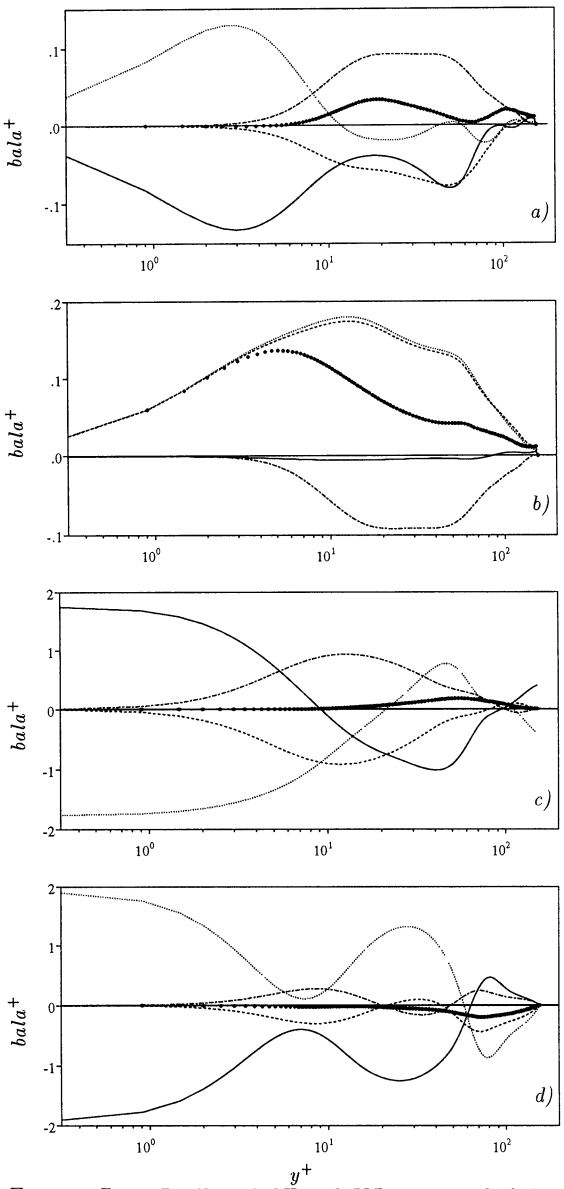

FIGURE 7. Profiles of CT and VP terms and their combination, in wall units (νu_τ^4), for $N = 2$ a) $< \overline{v_\theta' v_\theta'} >$, b) $< \overline{v_r' v_r'} >$, c) $< \overline{v_\theta' v_r'} >$, d) $< \overline{v_z' v_r'} >$ in function of y^+; (····· PD), (—— PS), (---- VP), (—-— CT), ($\bullet$ $PV + CT$).

The contribution of VP and CT in the equation for the turbulent stresses in Fig.7c-d shows, as an important feature, that the vertical scales are one order of magnitude greater than for the normal stresses. PS increases near the wall for effect of the rotation and, as for the non-rotating case, it is balanced by PD, this balance produces a small VP in the wall region, that at its turn is balanced by CT. Hence, even if each term is much larger, the contribution of both is of the same order than that in the normal stresses in Fig.7a-b. In the central region of the pipe $VP + CT$ counteracts the negative production . For $< \overline{v_z' v_r'} >$ the profiles do not change, there is an inversion of sign because for this stress $VP + CT$ balances the positive production.

This occurs also in the non-rotating case as it was shown by Mansour *et.al*(1988), we would like to point out that in the pipe some of the signs are opposite to those in the channel because in the pipe r is pointing towards the wall and in the channel y is pointing out from the wall.

CONCLUSIONS

The present study was performed in order to create a data-base for turbulent rotating pipes at a low Reynolds number and at low and high values of N. At the moment a satisfactory number of fields are available for $N = 0,\ 2,\ 5$ and 10 for $N = 0.5\ , 1$ the results were given by Fatica & Orlandi (1987); for several reason the fields were not saved and thus the balances were not calculated. The simulations do not take a long computational time and thus if someone has the interest to have the budgets at lower N we will appreciate to perform the simulations. Someone could argue that the data are not validated as for example those for the turbulent channel by Kim *et.al*(1987); we are aware of this, but it should be taken into consideration that this flow has a more complex flow physics. In addition the length of the pipe plays an important role and then a satisfactory streamwise resolution is difficult to achieve. We hope that in the near future other scholars will devote their time to perform the DNS of this flow by a different numerical method, as for instance that developed by Loulou (1996).

A set of validated data for this flow are very important because the steady solution by one-point closure requires only the discretization of a one-dimensional set of equations allowing the test of different closures. Despite the numerical simplicity the flow complexity remains which requires a satisfactory modeling. Only with the help of good results for the rotating pipe it will be possible to achieve satisfactory results in practical applications such as swirling jets.

REFERENCES

Durbin, P.A. 1991 "Near-wall turbulence closure modeling without damping functions". *Theor. Comp. Fluid Dyn.* **3**, 1–13

Ebstein, D. 1998 "Reynolds stresses and kinetic energy budgets in the flow through an axially rotating pipe" Fourth year Project of Aeronautical Engineering, Dept. of Aeronautics Imperial College, London

Eggels, J.G.M., Boersma, B.J. & Nieuwstadt, F.T.M. 1994 "Direct and large eddy simulations of turbulent flow in an axially rotating pipe flow". Preprint.

Hirai, S., Takagi, T. & Matsumoto, M. 1988 "Prediction of the laminarization phenomena in an axially rotating pipe flow" *Journal of Fluids Engineering,* **110**,424–430.

Imao, S., Itoh, M. & Harada, T. 1996 "Turbulent characteristics of the flow in axially rotating pipe" *Int. J. Heat & Fluid Flow* **17**, 444–451

Launder,B.E.,Reece,G.J. & Rodi,W. 1975 "Progress in the development of a Reynolds stress turbulence closure" *J.Fluid Mech,***67**,537–566.

Loulou, P. 1996 "Direct numerical simulation of incompressible pipe flow using a B-spline spectral method". Thesis Department of Aeronautics and Astronautics, SUDAAR 683, Stanford University.

Mansour, N.N. , Kim, J.& Moin, P. 1988" "Reynolds-stress and dissipation-rate budgets in a turbulent channel flow" *J.Fluid Mech,* **194**, 15–44.

Nishibori K., Kikuyama, K., & Murakami, M. 1987 "Laminarization of turbulent flow in the inlet region of an axially rotating pipe" JSME International Journal **30**,255–262.

Orlandi P. & Fatica, M. 1997 "Direct simulations of a turbulent pipe rotating along the axis" *J.Fluid Mech* ,**343**, 43–72.

Reich, G. & Beer, H. 1989 "Fluid flow and heat transfer in axially rotating pipe 1. Effect of rotation on turbulent pipe flow". *Intl. J. Heat Mass Transfer* **32**, 551–561

Rodi, W. & Mansour, N. 1993 "Low Reynolds number $k - \epsilon$ modelling with the aid of direct simulation data" *J.Fluid Mech,***250**, 509-529.

Verzicco, R. & Orlandi P. 1996 " A finite difference scheme for direct simulation in cylindrical coordinates" *J. of Comp. Phys,***123**,pp. 402-414.

Zeman, O. 1995 "The persistence of trailing vortices - a modeling study". *Phys. Fluids* **7**, 135–143